Microfluidic Generation of Particle-Stabilized Water-in-Water Emulsions

Niki Abbasi,[acd] *Maryam Navi,*[bcd] *and Scott. S. H. Tsai* [*abcd]

[a] Department of Mechanical and Industrial Engineering, Ryerson University, Toronto, Canada.

[b] Graduate Program in Biomedical Engineering, Ryerson University, Toronto, Canada.

[c] Keenan Research Centre for Biomedical Science, St. Michael's Hospital, Toronto, Canada.

[d] Institute for Biomedical Engineering, Science and Technology (iBEST) – a partnership between Ryerson University and St. Michael's Hospital.

Microfluidics, Emulsions, Aqueous-two-phase Systems, Stabilization

Address: Department of Mechanical and Industrial Engineering, Ryerson University, 350 Victoria Street, Toronto, ON, Canada, M5B 2K3

Email address of the corresponding author: scott.tsai@ryerson.ca

ABSTRACT

Herein, we present a microfluidic platform that generates particle-stabilized water-in-water emulsions. The water-in-water system that we use is based on an aqueous two-phase system of polyethylene glycol (PEG) and dextran (DEX). DEX droplets are formed passively, in the continuous phase of PEG and carboxylated particle suspension, at a flow focusing junction inside

a microfluidic device. As DEX droplets travel downstream inside the microchannel, carboxylated particles that are in the continuous phase partition to the interface of the DEX droplets, due to their affinity to the interface of PEG and DEX. As the DEX droplets become covered with carboxylated particles, they become stabilized against coalescence. We study the coverage and stability of the emulsions, while tuning the concentration and the size of the carboxylated particles, downstream inside the reservoir of the microfluidic device. These particle-stabilized water-in-water emulsions showcase good particle adsorption under shear, while being flowed through narrow microchannels. The intrinsic biocompatibility advantages of particle-stabilized water-in-water emulsions make them a good alternative to traditional particle-stabilized water-in-oil emulsions. To illustrate a biotechnological application of this platform, we show a proof-of-principle of cell encapsulation using this system, which with further development, may be used for immunoisolation of cells for transplantation purposes.

Introduction

Using colloidal particles to stabilize droplets against coalescence was first reported in the early 1900s.[1,2] Since then, particle-stabilized emulsions (so-called Pickering Emulsions) have been exploited in a variety of different fields. Some of the biotechnological applications of particle-stabilized emulsions include drug encapsulation and drug delivery.[3–5] The deposition of particles onto liquid-liquid interfaces is also utilized for the realization of new structures and materials. For example, hollow colloidosomes, based on water-in-oil emulsions, are produced to serve as immunoisolation agents,[6,7] and porous silica is made by using stabilized emulsions as a template.[8] Particle-stabilization of both oil-in-water and water-in-oil emulsions are studied

extensively, and particles based on iron,[9] protein,[10] silica,[11] latex,[12] and cellulose[13] are all effective stabilizing agents for oil-in-water and water-in-oil systems.

The conventional method of producing particle-stabilized emulsions is bulk emulsification, which involves mixing and stirring immiscible liquids with colloidal particles. This method of emulsification results in the generation of highly polydisperse droplets with different degrees of coverage, thus making it an unsuitable method for size-controlled emulsification.[14]

The advent of microfluidics in the past two decades is enabling the generation of highly monodisperse and functionalized water-in-oil and oil-in-water emulsions in a controlled fashion.[15–17] As a result, researchers are using microfluidics to generate monodisperse particle-stabilized emulsions.[18–20]

However, due to the toxicity of the organic oil phase, traditional particle-stabilized water-in-oil emulsions are not suitable for direct use in biotechnological applications, such as immunoisolation and drug delivery. An additional washing step is required to remove the oil phase from the particle-stabilized droplets, prior to their use.[6,21] For example, in the generation of hollow colloidosomes, the water-in-oil emulsions are washed and then transferred to an aqueous environment.[6] Although washing with an oil-soluble solution lightens the toxicity of the system, the shear stress caused by the washing flow may damage the assembly and the fine structure of the colloidal particles on the interface.[21]

Replacing the toxic organic continuous phase with a biocompatible fluid helps to eliminate the washing steps. This is a major reason why particle-stabilized water-in-water emulsions are desirable. Such water-in-water emulsions are based on aqueous-two-phase systems (ATPS), which are comprised of two incompatible polymeric aqueous solutions. ATPS have been

traditionally used as separation platforms for cells and macromolecules, based on their affinity partitioning and biocompatibility.[22] The mild environment of ATPS, which is due to their high water content, helps maintain the viability of biological samples.[23–26] The biocompatibility of ATPS makes them suitable candidates for making particle-stabilized emulsions for biotechnological applications.

Nevertheless, the ultra-low interfacial tension of ATPS makes it challenging to generate water-in-water emulsions using conventional microfluidic platforms, where syringe pumps are used to introduce the solutions.[27] As a result, a variety of active methods are proposed to realize microfluidic generation of water-in-water emulsions.[28–33] Recently, our group also introduced a passive microfluidic platform, that exploits the weak hydrostatic pressure difference of fluid columns from liquid-filled pipette tips inserted at the inlets of the dispersed and the continuous phases, to generate water-in-water droplets.[34]

In addition to generating water-in-water emulsions, realization of particle-stabilized water-in-water emulsions depends on the affinity of the selected particles to the fluid-fluid interface. The partitioning of particles within an ATPS depends highly on the surface interaction between the particles and the two aqueous phases. For example, emulsions of dextran-in-methylcellulose and dextran-in-polyethylene oxide can be stabilized by fat[21] and protein particles,[35,36] respectively, using bulk emulsification. Recently, Tsukamoto *et al.* reported affinity partitioning of carboxylated particles to the interface of an ATPS of polyethylene glycol (PEG) and dextran (DEX) within a microfluidic co-flow system.[37]

In this paper, we utilize our group's passive microfluidic platform,[34] and the recently demonstrated affinity partitioning of carboxylated particles in the ATPS of PEG and DEX,[37] to

generate particle-stabilized water-in-water emulsions. To the best of our knowledge, this is the first microfluidic implementation to generate particle-stabilized water-in-water emulsions. We make monodisperse DEX droplets at a flow focusing junction, in a continuous phase of PEG and carboxylated particles. As the DEX droplets travel downstream, carboxylated particles gradually cover the outer surface of the droplets by partitioning to the interface of the PEG and DEX phases. We study the effects of the size and concentration of the carboxylated particle suspension on the coverage and stability of the particle-stabilized DEX droplets. Finally, we show that the particle-stabilized water-in-water emulsions can be used to encapsulate cells, demonstrating the potential biotechnological application of this approach for cellular immunoisolation.

Experimental section

Chemicals

We follow the protocol developed by Atefi *et al.*[38] to prepare the ATPS. We prepare stock solutions of PEG 10 w/v% (PEG; M_w 35k, Sigma Aldrich, St. Louis, MO, USA) and DEX 12.8 w/v% (DEX, M_w 500k, Pharmacosmos, Holbaek, Denmark) in deionized (DI) water. We mix these two stock solutions together inside a Falcon™ tube (BD Medical, Franklin Lakes, NJ, USA) and let the mixture phase separate over a course of 24 hours. Then, the top phase (equilibrated PEG phase) and bottom phase (equilibrated DEX phase) are separated and transferred to separate Falcon™ tubes, using syringes (BD Medical, Franklin Lakes, NJ, USA). The interfacial tension of the ATPS, as reported by Atefi *et al.*,[38] is γ = 0.082 mN m^{-1}. The dynamic viscosities of the DEX and PEG phase are $\mu_{DEX} = 65.1$ mPa s and $\mu_{PEG} = 15.0$ mPa s, respectively.[39]

Microparticle suspension

To make our particle suspension, we use Polybead® carboxylate microsphere solutions of diameter d = 1, d = 6 and 10 µm (Polysciences, Inc., Warrington, PA, USA). Based on the particle solutions' data sheet, these carboxylated particles are negatively charged. We add 1 and 10 µL of the d = 1 µm diameter carboxylated microsphere, 10.8, 86.6, 108 and 173 µL of the d = 6 µm diameter carboxylated microsphere solution, and 50, 100, 200 and 600 µL of the d = 10 µm diameter carboxylated microsphere solution, to 1 mL of phase separated PEG inside a safe-lock tube (Eppendorf, Hamburg, Germany) separately. After vigorously mixing the particles with PEG, we centrifuge the particle suspensions and remove the carrier liquid using a pipette. Then, we add 1 mL of phase separated PEG to the washed carboxylated particles to complete the particle suspensions. These different microparticle suspensions are used in order to observe the effect microparticles' size and concentration on the coverage and the stability of the DEX droplets.

Cells

Acute Myeloid Leukemia (AML) cells are used in cell encapsulation experiments. Cells are cultured in Minimum Essential Medium (MEM) with 10% fetal bovine serum (FBS). After culture, cells are incubated inside a T-25 flask, at 37 °C with 5 % CO_2. After a day of incubation, cells are taken out from the T-25 flask (Thermo Scientific, Waltham, MA, USA) and transferred to a Falcon™ tube. Next, the cells are centrifuged to form a pellet at the bottom of the Falcon™ tube. Finally, after discarding the MEM solution, the cells are re-suspended in 1 mL of phase separated DEX solution.

Device fabrication

We use the standard soft lithography technique to make microfluidic devices.[40] To make a patterned photomask, we draw our microchannel design on a computer-aided design (CAD) software (AutoCAD 2016, Autodesk, Inc., San Rafael, CA, USA), and then the design is printed on a transparency sheet (CAD/ART Services Inc., Bandon, OR, USA).

We use a 4-inch diameter silicon wafer (UniversityWafer, Inc., Boston, MA, USA) to fabricate the microchannel features. We spin-coat SU-8 2050 photoresist (Microchem, Newton, MA, USA) on the silicon wafer. To create the microchannel patterns, we expose the spin-coated wafer to UV light through the patterned photomask. At the end, we remove the unexposed photoresist by washing the wafer with a developer solution, to complete the fabrication of the silicon master mold.

We fill the silicon master mold with a 10:1 ratio mixture of polydimethylsiloxane (PDMS) resin to curing agent (Sylgard 184, Dow Corning, Midland, MI, USA) and let it cure in an oven for 2 hours. Then, we cut the PDMS slab from the master, and we use 1 mm and 4 mm diameter biopsy punches (IntegraMiltex, Inc., Rietheim-Weilheim, Germany) for making inlets and outlet, respectively. To complete the device fabrication, we use oxygen plasma treatment (Harrick Plasma, Ithaca, NY, USA) in order to bond the PDMS slab to a glass slide.

Experimental Setup

Experimental images and videos are captured using an inverted microscope (IX71, Olympus Corp., Tokyo, Japan) with a connected high-speed camera (Miro M110, Vision Research, Wayne, NJ, USA) (Figure. 1 (a)). We use ImageJ^{TM} software to process videos and images.

We use our group's passive water-in-water droplet generation approach to infuse the liquids into the microfluidic device, and make emulsions.[34] DEX, and the suspension of carboxylated particles in PEG, are filled into separate 200 µL pipette tips, and subsequently inserted into their respective inlets on the microfluidic device (Figure 1(b)). The liquid column heights we use for DEX and the solution of PEG and suspended carboxylated particles are 2.5 and 3.5 cm, respectively. This set of column heights is selected to ensure hydrostatic pressures that cause generation of monodisperse DEX droplets in the dripping regime. The flow speed established is also low enough to lead to the partitioning of carboxylated particles to the surface of the DEX droplets within the microfluidic device.

As seen in Figure 1(c), the microfluidic device is comprised of two inlets and one outlet. The inlet channels converge at a flow focusing junction, and connect to the main channel through an orifice, which is 30 µm wide. The main channel, which is a long serpentine channel, is connected to a large circular reservoir near the outlet. All channel heights h = 50 µm. The flow of the DEX phase converges with the flow of the suspension of carboxylated particles in PEG, and DEX droplets with a diameter of D = 50 µm are generated (Figure 1(d)). As DEX droplets travel downstream through the serpentine channel, carboxylated particles in the continuous phase gradually partition to the outer surface of the DEX droplets.

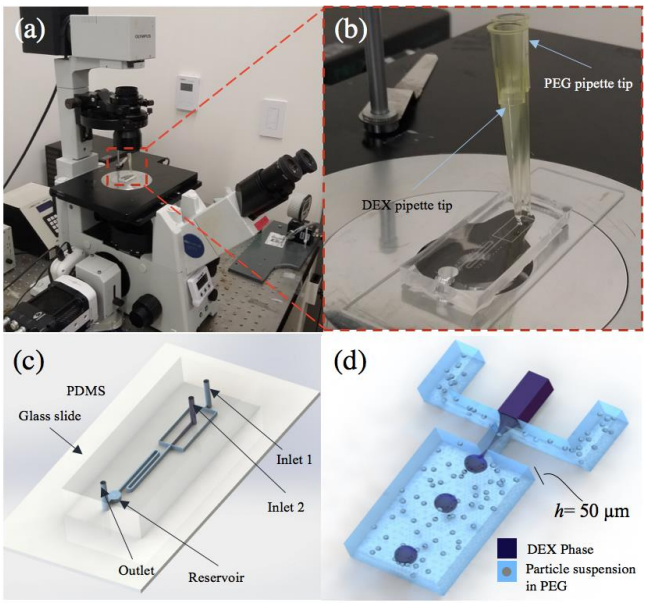

Figure 1. (a) An inverted microscope and a high-speed camera are used to monitor experiments and record videos. (b) Experimental setup of the microfluidic system, with pipette tips inserted at the inlets for infusion of the fluids into the chip. (c) Schematic diagram of the microfluidic device. A patterned PDMS slab is bonded to a glass slide, using a plasma chamber. (d) Schematic diagram of the flow-focusing junction of the microfluidic device. We generate the droplets at a flow-focusing junction with an orifice.

Results and discussion

Figure 2 shows time-series experimental images of particles partitioning to the interface of the DEX droplets, for different concentrations of d = 10 µm diameter carboxylated particles. We observe that, generally, particle coverage on the DEX droplets increases with the amount of time the droplets spend in the serpentine microchannel, and higher particle concentrations result in more complete droplet coverage. A time-series images of a DEX droplet becoming covered with d = 6 µm diameter carboxylated particles can be seen in the Supplementary Material, Figure S1. We also count the number of particles partitioning to the outer surface of the droplets, for

different particle sizes and different particle concentrations, from the moment the droplets are generated (which corresponds to time t = 0 s) until they reach the reservoir ($t \approx 450$ s). We describe the degree of droplet coverage $Nd^2/4D^2$, as the ratio of N, the number of particles partitioned to the droplet, to $4D^2/d^2$, the maximum number of particles that the surface area of the droplet can geometrically accommodate. Here, we assume that each carboxylated particle, of diameter d, covers a surface area equal to $\pi d^2/4$.

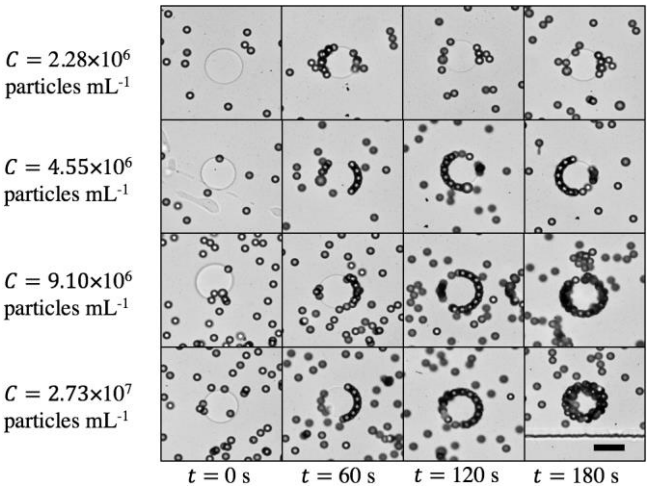

Figure 2. Time-series images of DEX droplets being covered with d = 10 μm diameter carboxylated particles, at different particle concentrations, in the serpentine region of the microfluidic device (see movie 1 in Supplementary Information). Higher particle concentrations result in faster coverage of the DEX droplets. Scale bar indicates 50 μm.

How well the carboxylated particles cover and remain on the interface of the DEX droplets is primarily affected by the competition between several physical phenomena. The binding energy or Gibbs desorption free energy $\Delta G = \gamma d^2(1 - cos\theta)^2/4$,[41] tends to keep the particles on the liquid-liquid interface. This energy is opposed by energies that try to pull the particles away from

the liquid-liquid interface, including the thermal energy kT, the Stoke's drag-based shear energy on the particle $6\pi\mu_{PEG}udD/2$, and the electrostatic repulsion energy between the charged carboxylated particles and the liquid-liquid interface. Here, θ is the contact angle between the liquid-liquid interface and the particle surface, Boltzmann's constant k = 1.38 × 10^{-23} m^2 kg s^{-2} K^{-1}, and temperature T = 293.15 K. The droplet flow speed u = 6.1 μm s^{-1} is kept constant in our experiments by careful tuning of the hydrostatic liquid column heights.

It is known that an electrostatic repulsion energy exists between charged particles and oil-water interfaces, which affects the partitioning of charged particles onto the interfaces.[20] This electrostatic repulsion increases with the difference in the dielectric constants of the two phases that form the liquid-liquid interface.[42] However, in our experiments with water-in-water emulsions, the carboxylated particles do not experience significant electrostatic repulsion forces from the liquid-liquid interface because the dielectric constants of both PEG and DEX phases, at such low polymer concentrations, are very close to that of water.[43,44] Therefore, we neglect electrostatic repulsion in our analysis.

To better understand how the remaining phenomena affect the ability of particles to remain on the liquid-liquid interface, we compare the orders-of-magnitude of each energy. Keeping the particles on the interface is the Gibbs free energy of desorption $\Delta G = O(10^{-18})$ J, where we assume that the two liquid phases have approximately the same degree of wetting on the particle surface, so the contact angle θ = 90º. In our experimental setup, the thermal energy $kT = O(10^{-21})$ J, and the shear energy on the particle $6\pi\mu_{PEG}udD/2 = O(10^{-18})$ J. Therefore, the thermal energy has a negligible effect on how well the carboxylated particles remain on the interface of the DEX droplets, and we find that the competition between the binding and shear energies is what decides whether partitioned particles stay on the interface of the water-in-water droplets.

Using an order-of-magnitude estimation, by equating the two most dominant energies, the shear energy $6\pi\mu_{PEG}udD/2$ and the binding energy $\gamma d^2(1-cos\theta)^2/4$,we find that the critical carboxylated particle diameter $d_c = O(1)$ μm, below which carboxylated particles do not stay attached to the droplet interface. Carboxylated particles that are smaller than $d_c = O(1)$ μm experience a higher shear energy than the binding energy and as a result, can easily get washed away from the surface of the DEX droplets. On the other hand, particles that have diameters greater than $d_c = O(1)$ μm possess higher binding energy, compared to shear energy. Therefore, they stay on the surface of the DEX droplets.

Figure 3 is a plot of the droplet coverage $Nd^2/4D^2$ versus the particle number concentration *C*. Based on the results shown on Figure 3, particles of both diameters d = 10 μm and d = 6 μm stay on the surface of DEX droplets. This observation is consistent with the order-of-magnitude estimation of the critical particle diameter, $d_c = O(1)$ μm, above which particles remain on the interface. We find that the droplet coverage increases monotonically with particle concentration for both particle sizes. As particle concentration increases, the chance of a particle colliding with the surface of the DEX droplets increases. The increase in particle-interface collisions increases the coverage of the DEX droplets.

Moreover, using larger d = 10 μm diameter particles results in better coverage, compared to stabilizing with the smaller d = 6 μm diameter particles. The lower DEX droplet coverage obtained with d = 6 μm diameter particles is an indication that this particle diameter is near the critical particle diameter d_c, below which shear stresses overcome the particle-interface binding energy, and particles detach from the droplet interface more easily.

We also use d = 1 μm diameter carboxylated particles with particle number concentration C = 4.55×10^7 particles mL^{-1} and C = 4.55×10^8 particles mL^{-1}, and in these experiments, we do not observe any particles remaining on the interface of the DEX droplets. Those particles that interact with the surface of the DEX droplets are washed away soon after, indicating that the shear energy on the particles is greater than the particles' binding energy to the DEX droplet interface (see Supplementary Information movie 2). This observation further demonstrates that the actual value of the critical carboxylated particle diameter, d_c, lies between 1 – 6 μm.

We note that, in our microfluidic geometry, the DEX droplets cannot achieve a complete droplet coverage $Nd^2/4D^2 = 1$, because the generated droplet diameter D is the same as the channel height h. Since the carboxylated particles cannot partition to areas of the droplet that are in contact with the PDMS (i.e. the top and bottom surfaces), we observe a maximum droplet coverage $Nd^2/4D^2 \approx 0.75$.

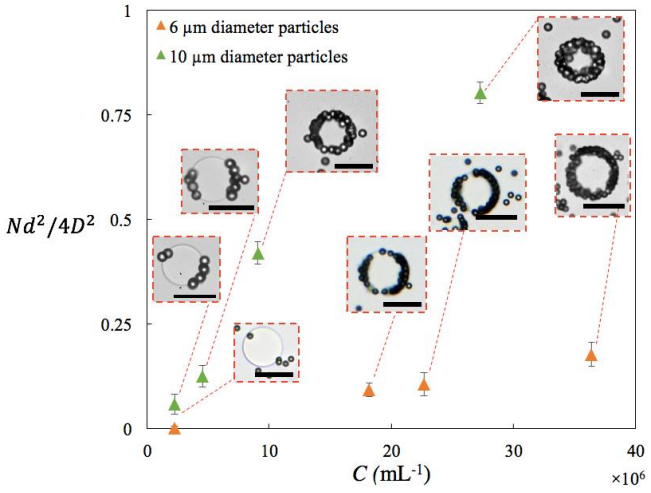

Figure 3. Plot of droplet coverage $Nd^2/4D^2$ versus carboxylated particle number concentration C in the PEG phase. The coverage of the DEX droplets increases with the particle concentration and particle size. Scale bars indicate 50 μm.

We flow the DEX droplets into a large reservoir in our microfluidic device (see Figure 1) to quantify the ability of the particle-stabilized droplets to withstand coalescence. As the DEX droplets enter the reservoir, they slow down and as a result, droplets come in contact with one another. We measure the reservoir entering droplet diameter, D_i, and compare with the reservoir exiting droplet diameter, D_f, to quantify the amount of coalescence taking place in the reservoir. The DEX droplets travel inside the reservoir for about t = 450 s.

Figure 4(a) shows a plot of the diameter ratio, D_f/D_i, versus the coverage $Nd^2/4D^2$. As the coverage of the DEX droplets increases, D_f/D_i decreases, meaning that the droplets are becoming stable against coalescence and preserving their size. Figure 4(b) shows that for a given particle concentration, larger particle size results in lower incidences of coalescence.

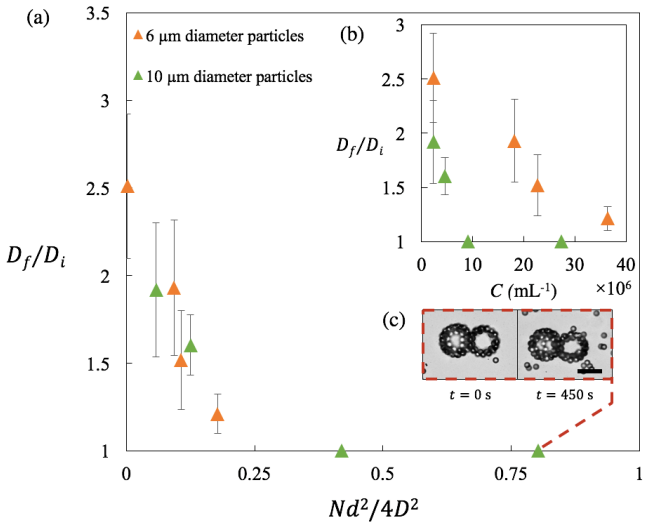

Figure 4. (a) Plot of the final to initial droplet diameter ratio D_f/D_i versus droplet coverage $Nd^2/4D^2$. As expected, an increase in droplet coverage $Nd^2/4D^2$ results in a decrease in the diameter ratio D_f/D_i indicating that droplets become stabilized against coalescence. (b) Plot of

the final to initial droplet diameter D_f/D_i versus particle concentration C. We observe that larger particles at higher concentration are more effective in droplet stabilization. (c) Inset shows a time-series of images of two particle-stabilized DEX droplets inside the reservoir of the microfluidic device. Despite being in contact over the course of 450 s, the two droplets do not coalesce. Scale bar indicates 50 µm.

These particle-stabilized water-in-water emulsions also exhibit the ability to retain particle coverage under shear. Figure 5 shows a time-series of images of a single particle-stabilized emulsion squeezing through a small microchannel construction, inside the reservoir of the microfluidic device. Despite the low free energy of desorption of the particles, only a small number of particles desorb from the DEX droplet surface while the droplet squeezes through the constriction. The particle aggregation observed in Figure 5 can be attributed to the binding energy between the particles, as a result of the presence of PEG molecules inside the particle suspension.[45]

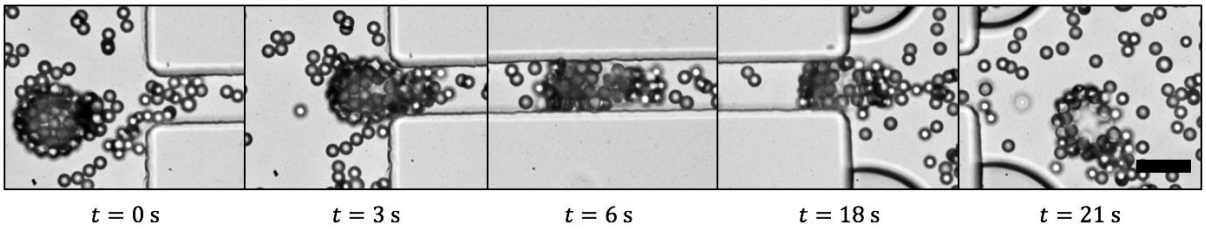

Figure 5. Time-series images of a particle-stabilized DEX droplet squeezing and flowing through a narrow constriction, which is located inside the reservoir of the microfluidic device. Stabilizing particles have diameter d = 10 µm. Most particles remain on the droplet as the droplet exits the narrow constriction and return to a spherical shape. The scale bar indicates 50 µm.

As a proof-of-concept example of the biotechnological application of this system, we encapsulate AML cells using this platform, in a water-in-water DEX droplet that is stabilized by d = 10 μm diameter carboxylated particles. Figure 6 shows the encapsulation of an AML cell inside a particle-stabilized DEX droplet. The biocompatibility of these ATPS-based particle-stabilized emulsions make them a good alternative to water-in-oil emulsions for cell-encapsulation and immunoisolation purposes, and other biotechnological applications. Based on our AML cells viability studies (which can be found in the Supplementary Material, Figure S2), the presence of DEX does not impinge on the viability of the AML cells.

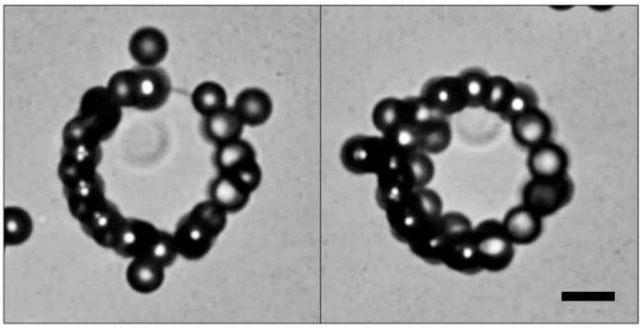

Figure 6. Time series images of a single particle- stabilized DEX droplet encapsulating an AML cell. The particles are 10 μm in diameter. Scale bar indicates 20 μm.

Conclusions

We present a microfluidic platform that enables the generation and stabilization of water-in-water emulsions, using carboxylated particles. We utilize a flow-focusing microfluidic device to generate water-in-water emulsions of DEX-in-PEG. Carboxylated particles that are suspended in the continuous phase of PEG gradually partition to the outer surface of DEX droplets, and over

time, they cover the droplets. Changes in the particle size and the particle concentration affect the coverage and stability of the DEX droplets. Owing to their intrinsic biocompatibility, particle- stabilized water-in-water emulsions are a good alternative for traditional particle-stabilized water-in-oil emulsions. These emulsions could be utilized in a variety of biotechnological applications, such as cell encapsulation and drug delivery.

ASSOCIATED CONTENT

Supporting Information

The Supporting Information is available free of charge on the ACS Publications website.

Figures S1 and S2.

Movie 1

Movie 2

AUTHOR INFORMATION

Corresponding Author

* Email: scott.tsai@ryerson.ca

ACKNOWLEDGMENT

The authors acknowledge A. Salari and the laboratory of M. C. Kolios for supplying the AML cells that are used in the cell encapsulation experiments. S. S. H. Tsai is also grateful for funding support from the Canadian Natural Sciences and Engineering Research Council (NSERC) Discovery grants program (grant no. 435514-2013), as well as Ontario's Ministry of Research, Innovation, and Science (MRIS) Early Researcher Award (grant no. ER15-11-163).

REFERENCES

(1) Ramsden, W. Separation of Solids in the Surface-Layers of Solutions and "Suspensions" (Observations on Surface-Membranes, Bubbles, Emulsions, and Mechanical Coagulation). *Proc. R. Soc. L.* **1903**, *72*, 156–164.

(2) Pickering, S. U. Pickering: Emulsions. *J. Chem. Soc. Trans.* **1907**, *91*, 2001–2021.

(3) Simovic, S.; Prestidge, C. A. Pickering Emulsions for Dermal Delivery. *J. Drug Deliv. Sci. Technol.* **2011**, *21*, 123–133. Available from: doi: 10.1016/S1773-2247(11)50011-5

(4) Frelichowska, J.; Bolzinger, M. A.; Valour, J. P.; Mouaziz, H.; Pelletier, J.; Chevalier, Y. Pickering W/O Emulsions: Drug Release and Topical Delivery. *Int. J. Pharm.* **2009**, *368*, 7–15. Available from: doi: 10.1016/j.ijpharm.2008.09.057

(5) Frelichowska, J.; Bolzinger, M. A.; Pelletier, J.; Valour, J. P.; Chevalier, Y. Topical Delivery of Lipophilic Drugs from O/W Pickering Emulsions. *Int. J. Pharm.* **2009**, *371*, 56–63. Available from: doi: 10.1016/j.ijpharm.2008.12.017

(6) Dinsmore, A. D.; Hsu, M. F.; Nikolaides, M. G.; Marquez, M.; Bausch, A. R.; Weitz, D. A. Colloidosomes : Selectively Permeable Capsules Composed of Colloidal Particles. *Science* **2002**, *298*, 1006–1009. Available from: doi: 10.1126/science.1074868

(7) Lee, D.; Weitz, D. A. Nonspherical Colloidosomes with Multiple Compartments from Double Emulsions. *Small* **2009**, *5*, 1932–1935. Available from: doi: 10.1002/smll.200900357

(8) Binks, B. P. Macroporous Silica From Solid-Stabilized Emulsions Templates. *Adv. Mater.* **2002**, *14*, 1824–1827. Available from: doi: 10.1002/adma.200290010

(9) Zhou, J.; Qiao, X.; Binks, B. P.; Sun, K.; Bai, M.; Li, Y.; Liu, Y. Magnetic Pickering Emulsions Stabilized by Fe_3O_4 Nanoparticles. *Langmuir* **2011**, *27*, 3308–3316. Available from: doi: 10.1021/la1036844

(10) de Folter, J. W. J.; van Ruijven, M. W. M.; Velikov, K. P. Oil-in-Water Pickering Emulsions Stabilized by Colloidal Particles from the Water-Insoluble Protein Zein. *Soft Matter* **2012**, *8*, 6807–6815. Available from: doi: 10.1039/C2SM07417F

(11) Vignati, E.; Piazza, R.; Lockhart, T. P. Pickering Emulsions: Interfacial Tension, Colloidal Layer Morphology, and Trapped-Particle Motion. *Langmuir* **2003**, *19*, 6650–6656. Available from: doi: 10.1021/la034264l

(12) Binks, B. P.; Lumsdon, S. O. Pickering Emulsions Stabilized by Monodisperse Latex Particles : Effects of Particle Size. *Langmuir* **2001**, *17*, 4540–4547. Available from: doi: 10.1021/la0103822

(13) Wege, H. A.; Kim, S.; Paunov, V. N.; Zhong, Q.; Velev, O. D. Long-Term Stabilization of Foams and Emulsions with In-Situ Formed Microparticles from Hydrophobic Cellulose. *Langmuir* **2008**, *24*, 9245–9253. Available from: doi: 10.1021/la801634j

(14) Huebner, A.; Sharma, S.; Srisa-Art, M.; Hollfelder, F.; Edel, J. B.; DeMello, A. J. Microdroplets : A Sea of Applications? *Lab Chip* **2008**, *8*, 1244–1254. Available from: doi: 10.1039/B806405A

(15) Thorsen, T.; Roberts, R. W.; Arnold, F. H.; Quake, S. R. Dynamic Pattern Formation in a Vesicle-Generating Microfluidic Device. *Phys. Rev. Lett.* **2001**, *86*, 4163–4166. Available from: doi: 10.1103/PhysRevLett.86.4163

(16) Anna, S. L.; Bontoux, N.; Stone, H. A. Formation of Dispersions Using "'flow Focusing'" in Microchannels. *Appl. Phys. Lett.* **2003**, *82*, 364–366. Available from: doi: 10.1063/1.1537519

(17) Wang, W.; Zhang, M. J.; Chu, L. Y. Functional Polymeric Microparticles Engineered from Controllable Microfluidic Emulsions. *Acc. Chem. Res.* **2014**, *47* (2), 373–384. Available from: doi: 10.1021/ar4001263
(18) Nie, Z.; Park, J. I.; Li, W.; Bon, S. A. F.; Kumacheva, E. An "inside-out" Microfluidic Approach to Monodisperse Emulsions Stabilized by Solid Particles. *J. Am. Chem. Soc.* **2008**, *130*, 16508–16509. Available from: doi: 10.1021/ja807764m
(19) Priest, C.; Reid, M. D.; Whitby, C. P. Formation and Stability of Nanoparticle-Stabilised Oil-in-Water Emulsions in a Microfluidic Chip. *J. Colloid Interface Sci.* **2011**, *363*, 301–306. Available from: doi: 10.1016/j.jcis.2011.07.060
(20) Subramaniam, A. B.; Abkarian, M.; Stone, H. A. Controlled Assembly of Jammed Colloidal Shells on Fluid Droplets. *Nat. Mater.* **2005**, *4*, 553–556. Available from: doi: 10.1038/nmat1412
(21) Poortinga, A. T. Microcapsules from Self-Assembled Colloidal Particles Using Aqueous Phase-Separated Polymer Solutions. *Langmuir* **2008**, *24*, 1644–1647. Available from: doi: 10.1021/la703441e
(22) Albertsson, P. A. Chromatography and Partition of Cells and Cell Fragments. *Nature* **1956**, *177*, 771–774. Available from: doi: 10.1038/177771a0
(23) Hardt, S.; Hahn, T. Microfluidics with Aqueous Two-Phase Systems. *Lab Chip* **2012**, *12*, 434–442. Available from: doi: 10.1039/C1LC20569B
(24) Grilo, A. L.; Aires-Barros, M. R.; Azevedo, A. M. Partitioning in Aqueous Two-Phase Systems: Fundamentals, Applications and Trends. *Sep. Purif. Rev.* **2016**, *45*, 68–80. Available from: doi: 10.1080/15422119.2014.983128
(25) Song, Y.; Chan, Y. K.; Ma, Q.; Liu, Z.; Shum, H. C. All-Aqueous Electrosprayed Emulsion for Templated Fabrication of Cytocompatible Microcapsules. *ACS Appl. Mater. Interfaces* **2015**, *7*, 13925–13933. Available from: doi: 10.1021/acsami.5b02708
(26) Han, C.; Takayama, S.; Park, J. Formation and Manipulation of Cell Spheroids Using a Density Adjusted PEG/DEX Aqueous Two Phase System. *Sci. Rep.* **2015**, *5*, 1–11. Available from: doi: 10.1038/srep11891
(27) Geschiere, S. D.; Ziemecka, I.; van Steijn, V.; Koper, G. J. M.; van Esch, J. H.; Kreutzer, M. T. Slow Growth of the Rayleigh-Plateau Instability in Aqueous Two Phase Systems. *Biomicrofluidics* **2012**, *6*, 22007-1–11. Available from: doi: 10.1063/1.3700117
(28) Shang, L.; Cheng, Y.; Zhao, Y. Emerging Droplet Microfluidics. *Chem. Rev.* **2017**, *117*, 7964–8040. Available from: doi: 10.1021/acs.chemrev.6b00848
(29) Song, Y. S.; Choi, Y. H.; Kim, D. H. Microextraction in a Tetrabutylammonium Bromide/ammonium Sulfate Aqueous Two-Phase System and Electrohydrodynamic Generation of a Micro-Droplet. *J. Chromatogr. A* **2007**, *1162*, 180–186. Available from: doi: 10.1016/j.chroma.2007.06.032
(30) Ziemecka, I.; van Steijn, V.; Koper, G. J. M.; Rosso, M.; Brizard, A. M.; van Esch, J. H.; Kreutzer, M. T. Monodisperse Hydrogel Microspheres by Forced Droplet Formation in Aqueous Two-Phase Systems. *Lab Chip* **2011**, *11*, 620–624. Available from: doi: 10.1039/C0LC00375A
(31) Lai, D.; Frampton, J. P.; Sriram, H.; Takayama, S. Rounded Multi-Level Microchannels with Orifices Made in One Exposure Enable Aqueous Two-Phase System Droplet Microfluidics. *Lab Chip* **2011**, *11*, 3551–3554. Available from: doi: 10.1039/C1LC20560A

(32) Shum, H. C.; Varnell, J.; Weitz, D. A. Microfluidic Fabrication of Water-in-Water (W/W) Jets and Emulsions. *Biomicrofluidics* **2012**, *6*, 12808-1–9. Available from: doi: 10.1063/1.3670365
(33) Moon, B.; Jones, S. G.; Hwang, D. K.; Tsai, S. S. H. Microfluidic Generation of Aqueous Two-Phase System (ATPS) Droplets by Controlled Pulsating Inlet Pressures. *Lab Chip* **2015**, *15*, 2437–2444. Available from: doi: 10.1039/C5LC00217F
(34) Moon, B.; Abbasi, N.; Jones, S. G.; Hwang, D. K.; Tsai, S. S. H. Water-in-Water Droplets by Passive Microfluidic Flow Focusing. *Anal. Chem.* **2016**, *88*, 3982–3989. Available from: doi: 10.1021/acs.analchem.6b00225
(35) Balakrishnan, G.; Nicolai, T.; Benyahia, L.; Durand, D. Particles Trapped at the Droplet Interface in Water-in-Water Emulsions. *Langmuir* **2012**, *28*, 5921–5926. Available from: doi: 10.1021/la204825f
(36) Nguyen, B. T.; Nicolai, T.; Benyahia, L. Stabilization of Water-in-Water Emulsions by Nanorods. *Langmuir* **2013**, *29*, 10658–10664. Available from: doi: 10.1021/acsmacrolett.5b00953
(37) Tsukamoto, M.; Taira, S.; Yamamura, S.; Morita, Y.; Nagatani, N.; Takamura, Y.; Tamiya, E. Cell Separation by an Aqueous Two-Phase System in a Microfluidic Device. *Analyst* **2009**, *134*, 1994–1998. Available from: doi: 10.1039/B909597G
(38) Atefi, E.; Mann, J. A.; Tavana, H. Ultralow Interfacial Tensions of Aqueous Two-Phase Systems Measured Using Drop Shape. *Langmuir* **2014**, *30*, 9691–9699. Available from: doi: 10.1021/la500930x
(39) Jones, S. G.; Abbasi, N.; Moon, B.-U.; Tsai, S. S. H. Microfluidic Magnetic Self-Assembly at Liquid-Liquid Interfaces. *Soft Matter* **2016**, *12*, 2668–2675. Available from: doi: 10.1039/C5SM03104D
(40) Xia, Y.; Whitesides, G. M. Soft Lithography. *Annu. Rev. Mater. Sci.* **1998**, *28*, 153–184. Available from: doi: 10.1146/annurev.matsci.28.1.153
(41) Firoozmand, H.; Murray, B. S.; Dickinson, E. Interfacial Structuring in a Phase-Separating Mixed Biopolymer Solution Containing Colloidal Particles. *Langmuir* **2009**, *25*, 1300–1305. Available from: doi: 10.1021/la8037389
(42) Mbamala, E. C.; Grünberg, H. H. Von. Effective Interaction of a Charged Colloidal Particle with an Air-Water Interface. *J. Phys. Condens. Matter* **2002**, *14*, 4881–4900. Available from: doi: 10.1088/0953-8984/14/19/313
(43) Arnold, K.; Herrmann, A.; Pratsch, L.; Gawrisch, K. The Dielectric Properties of Aqueous Solutions of Poly(ethylene Glycol) and Their Influence on Membrane Structure. *Biochim. Biophys. Acta - Biomembr.* **1985**, *815*, 515–518. Available from: doi: 10.1016/0005-2736(85)90381-5
(44) Zaslavsky, B. Y.; Miheeva, L. M.; Rodnikova, M. N.; Spivak, G. V.; Harkin, V. S.; Mahmudov, A. U. Dielectric Properties of Water in the Coexisting Phases of Aqueous Polymeric Two-Phase Systems. *J. Chem. Soc. Faraday Trans. 1 Phys. Chem. Condens. Phases* **1989**, *85*, 2857–2865. Available from: doi: 10.1039/F19898502857
(45) La Mer, V. K.; Healy, T. W. The Role of Filtration in Investigating Flocculation and Redispersion of Colloidal Dispersions. *J. Phys. Chem.* **1963**, *67*, 2417–2420. Available from: doi: 10.1021/j100805a038

Graphical TOC Entry